Fuel cell electric vehicle as a power plant and SOFC as a natural gas reformer
An exergy analysis of different system designs

Fernandes, A.; Woudstra, T.; van Wijk, A.; Verhoef, L.; Purushothaman Vellayani, A.

DOI
10.1016/j.apenergy.2016.03.107

Publication date
2016

Document Version
Final published version

Published in
Applied Energy

Applied Energy 173 (2016) 13–28

Contents lists available at ScienceDirect

Applied Energy

journal homepage: www.elsevier.com/locate/apenergy

Fuel cell electric vehicle as a power plant and SOFC as a natural gas reformer: An exergy analysis of different system designs

A. Fernandes [a,*], T. Woudstra [a], A. van Wijk [a], L. Verhoef [b], P.V. Aravind [a]

[a] Energy Technology Section, Department of Process and Energy, Delft University of Technology, Leeghwaterstraat 39, 2628 CB Delft, The Netherlands
[b] New-Energy-Works®, Hooghiemstraplein 160, 3514 AZ Utrecht, The Netherlands

HIGHLIGHTS

- A novel concept of a trigeneration plant using fuel cell vehicles is presented.
- Energy and water production based on FCEVs studied.
- Internal reforming SOFCs are compared with catalytic reformers.
- Efficiency penalties with CCS are presented.

ARTICLE INFO

Article history:
Received 4 December 2015
Received in revised form 22 March 2016
Accepted 29 March 2016
Available online 9 April 2016

Keywords:
SOFC
Reforming
Vehicle-to-grid (V2G)
Exergy
Trigeneration

ABSTRACT

Delft University of Technology, under its "Green Village" programme, has an initiative to build a power plant (car parking lot) based on the fuel cells used in vehicles for motive power. It is a trigeneration system capable of producing electricity, heat, and hydrogen. It comprises three main zones: a hydrogen production zone, a parking zone, and a pump station zone. This study focuses mainly on the hydrogen production zone which assesses four different system designs in two different operation modes of the facility: Car as Power Plant (CaPP) mode, corresponding to the open period of the facility which uses fuel cell electric vehicles (FCEVs) as energy and water producers while parked; and Pump mode, corresponding to the closed period which compresses the hydrogen and pumps to the vehicle's fuel tank. These system designs differ by the reforming technology: the existing catalytic reformer (CR) and a solid oxide fuel cell operating as reformer (SOFCR); and the option of integrating a carbon capture and storage (CCS).

Results reveal that the SOFCR unit significantly reduces the exergy destruction resulting in an improvement of efficiency over 20% in SOFCR-based system designs compared to CR-based system designs in both operation modes. It also mitigates the reduction in system efficiency by integration of a CCS unit, achieving a value of 2% whereas, in CR-based systems, is 7–8%. The SOFCR-based system running in Pump mode achieves a trigeneration efficiency of 60%.

1. Introduction

The energy deficit caused by importing fossil fuels as a primary energy resource conjointly with the need to reduce greenhouse gas emissions led the European Union (EU) to define new energy policies for the following decades. These include a reduction of greenhouse gas emissions of 25% and 80% by 2020 and 2050, respectively, when compared to 1990 [1]. In 2010, 64% of fossil fuels and 2.4% of electricity were consumed in the transportation sector which represents 32% of the total energy consumption in EU. From this energy, 80% is used in road transportation [2]. As a result, a decarbonisation transition of the transportation sector will be conducted in the forthcoming decades. It will be done primarily by improvement in energy efficiency on existing technologies as well as the integration of new technologies in power systems of vehicles and, secondly, by integration of carbon capture and storage units (CCS) in fuel and electricity production plants, and finally to a transition to a massive fuel production and energy from renewable energy sources [3]. Additionally, the intermittent nature of renewable energy sources will also require massive changes in electricity network: flexibility in demand, electricity storage, electricity conversion into fuels, chemicals or heat, and smart grids needs to be developed.

* Corresponding author.
E-mail addresses: A.B.MonteiroFernandes@tudelft.nl (A. Fernandes), T.Woudstra@tudelft.nl (T. Woudstra), a.j.m.vanwijk@tudelft.nl (A. van Wijk), L.Verhoef@new-energy-works.com (L. Verhoef), PV.Aravind@tudelft.nl (P.V. Aravind).

http://dx.doi.org/10.1016/j.apenergy.2016.03.107
0306-2619/

Nomenclature

Abbreviations

Air PH	air pre-heater
BEV	battery electric vehicle
CaPP	Car as Power Plant
CCS	carbon capture and storage
CR	catalytic reformer
CW	cooling water
ECO	economizer
EU	European Union
FCEV	fuel cell electric vehicle
HRSG	heat recovery steam generator
HTS	high temperature shift reactor
HW	hot water
ICEV	internal combustion engine vehicle
LTS	low temperature shift reactor
MCFC	molten carbonate fuel cell
PEMFC	polymer exchange membrane fuel cell
PSA	pressure swing adsorption
SH	super heater
SMR	steam methane reforming
SOFC	solid oxide fuel cell
SOFCR	solid oxide fuel cell as a reformer
WT Mng	water management
WT Sep	water separator

Subscripts

*i*th	component *i*th in a mixture
j	*j*-th product
aux	auxiliary components
in	inlet
mode	operation mode
NG	natural gas
out	outlet

Variables

η	energy efficiency (%)
η_{is}	isentropic efficiency (%)
R_{eq}	area specific resistance ($\Omega\,cm^2$)
$\overline{h}$	specific enthalpy (kJ/mol)
$\overline{s}$	specific entropy (kJ/(mol K))
$\dot{W}$	electricity (kW)
$\dot{E}$	exergy flow (kW)
$\dot{E}_d$	exergy destruction (kW)
Φ_{mol}	mole flow, mole per second (mol/s)
$\Delta Time$	operational time in the mode (h)
ε	exergy efficiency (%)
e	specific energy (kJ/mol)
f_{ex}	exergy factor (–)
LHV	lower heating value (kJ/kg)
p	pressure (Pa)
RH	relative humidity (%)
S/C	steam to carbon ratio (mol/mol)
T	temperature (K)
U_f	fuel utilization (mol/mol)
U_{ox}	oxidant utilization (mol/mol)
V	voltage (V)
y	mole fraction

A study funded by the European Commission remarks that only vehicles powered by carbon-free fuels or electricity can accomplish the target of reduction in greenhouse gas emissions by 2050. It was also reported that a large penetration of vehicles other than existing internal combustion engine vehicles (ICEVs) is crucial due to the limited enhancement in the efficiency of these vehicles. Additionally, fuel production should also meet the targets in the reduction of carbon emissions [3].

Therefore, batteries and fuel cells combined with electric motors are in the forefront to substitute the internal combustion engine. Nevertheless, batteries only present a solution if utilized alone or in hybrid systems fueled by carbon-free fuels. Additionally, two aspects are limiting a large penetration of battery powered vehicles (BEVs) on the market: low driving range and long charging time [4]. In contrast, FCEVs do not have such limitations and, therefore, can meet similar driving ranges as ICEVs [5].

Market introduction of FCEVs is now starting and the penetration is expected to be substantial in the future [3]. First steps are being taken by car manufacturers who have been developing FCEVs such as Hyundai, Toyota, Ford, Daimler, and Nissan [6–8] among others. Additionally, a programme to install 400 hydrogen fueling stations by 2023 in Germany is undergoing [9]. Also, the Japanese government wants to create a market for hydrogen and fuel cell cars, with projected annual market size increasing to 400,000 FCEVs in 2030 [10].

The low average operating time of a vehicle, slightly above 1 h/day [11,12], along with the capability of these vehicles for storing and supplying energy has led to investigations on their integration in the stationary energy systems (also called vehicle-to grid, V2G). Current studies are mainly focused on analyzing the interaction with and impact on the electric grid network [13,14], charging models [15,16], battery degradation [17,18] when using BEVs and PHEV as energy storage units to regulate the fluctuating nature of the electric grid [19] as well as economic and environmental benefits [20,21] are certain examples. Nevertheless, other studies also state that a large penetration on the market of BEVs and PHEVs will also increase the electric power demand. Ideally, it should be covered by renewable energy sources to limit carbon emissions. However, in some particular cases, this cannot be achieved due to limited production capacity of several countries. Therefore, new coal power plants are suggested [22].

FCEVs are also considered as appropriate for stationary power production [23–27]. In this way, the increase in power demand could be covered by small and medium scale decentralized combined heat and power units. These would also increase overall energy efficiency of the electric grid: highly efficient electricity production and reduction in transmission losses. In addition, capital and maintenance costs in transmission networks are also reduced [28].

Kempton et al. concluded that the utilization of FCEVs for electricity production is more economically beneficial if hydrogen is produced by large capacity natural gas steam reforming-based plants [27]. The low capital and operation costs per kg of hydrogen produced as well as the higher efficiency is pivotal for the reduction of the hydrogen price in the market. The efficiency can even be improved by replacing of the current catalytic reformer by emerging technologies such as high temperature fuel cells. Molten carbonate fuel cells (MCFC) and solid oxide fuel cells are being investigated as a natural gas reformer for high purity hydrogen production [29–31]. These aspects already led to the development and construction of these novel hydrogen production plants [32,33].

A novel infrastructure, known as "Car as Power Plant" or "Car Park Power Plant", is an innovative example of a FCEV-based CHP plant (Fig. 1). Detailed information and progress status can be found in Appendix A. It functions as a car parking garage, however,

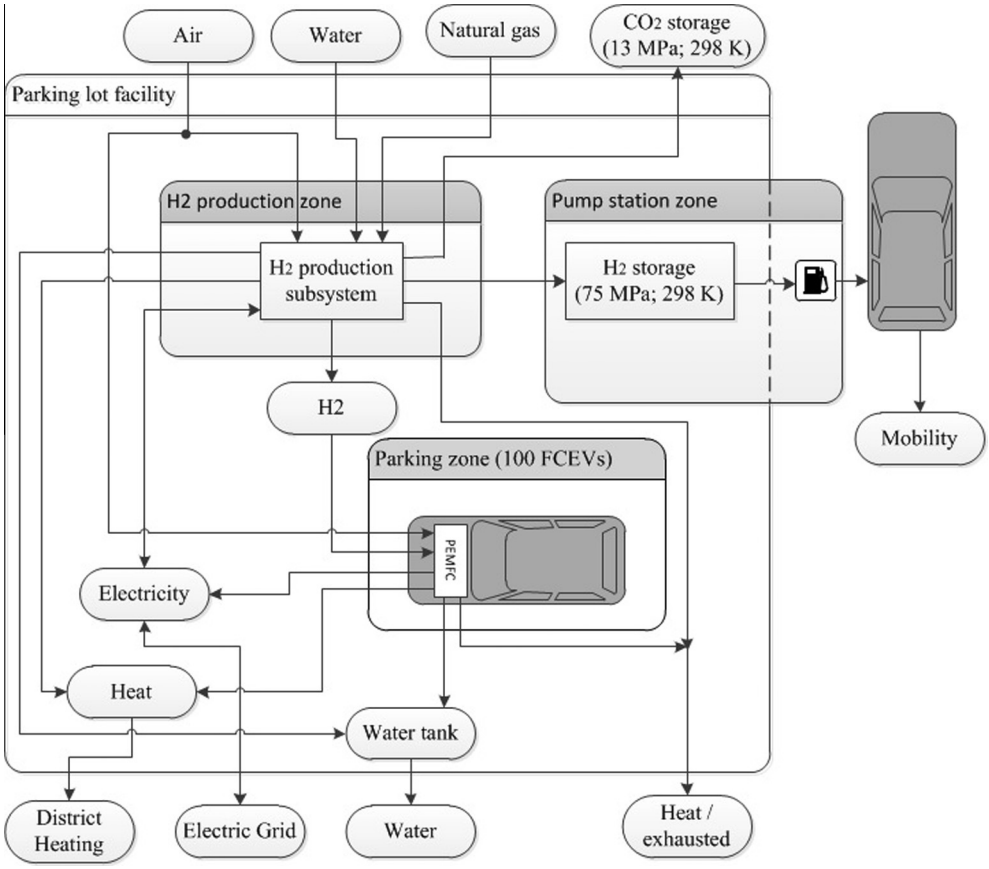

Fig. 1. Layout of the "Car as Power Plant" Facility and flow diagram of inlet and outlet streams.

it introduces the concept of a trigeneration plant. It integrates of a hydrogen production subsystem through natural gas reforming to enable the production of electricity, heat, and water by the FCEVs as well as hydrogen to be used in an external pump station. The "Car as Power Plant" concept is getting increasingly attractive, and TU Delft, in partnership with various prestigious international companies, has started an initiative to build such a novel plant on its campus. The recent book entitled "Our Car as Power Plant" authored by van Wijk and Verhoef provides the details [34]. They envision this infrastructure " ...with capability to create an integrated, efficient, reliable, flexible, clean, smart and personalized transport – energy – and water system". In addition, SOFCs acting as reformers for hydrogen production potentially make these plants compete with natural gas combined cycle plants in efficiency and cost aspects due to the use of existing power units (FCEVs). Currently, large scale natural gas combined cycle plants (>50 MWe) can achieve efficiencies up to 61%. In future, these plants are expected to achieve an efficiency of 65% by increasing the inlet gas temperature to 1973 K [35]. Nevertheless, in contrast to fuel cell systems, two different points are to be noted: low efficiency at small scales (<50 MWe) and part-loads [36].

To the best of acknowledge of others, this paper, for the first time, presents detailed thermodynamic calculations showing the achievable efficiencies when FCEVs are used as power plants. This study includes: (1) conceptual process flow schemes for a natural gas based CAPP facility, (2) detailed analysis of energy and exergy flows in such units, (3) comparison between different reforming technologies for hydrogen production for such systems, and (4) evaluates the influence of carbon capture on achievable efficiencies.

It is conducted through a modeling work to thermodynamically assess four different system designs for the hydrogen production plant is carried out. It aims to determine the most efficient system design. Electricity, mobility, heat, and water are the products obtained. All four system designs employ a similar flow process as described in Fig. 2: a desulfurizer, a reformer, a water gas shift unit (WGS), and a hydrogen purification unit.

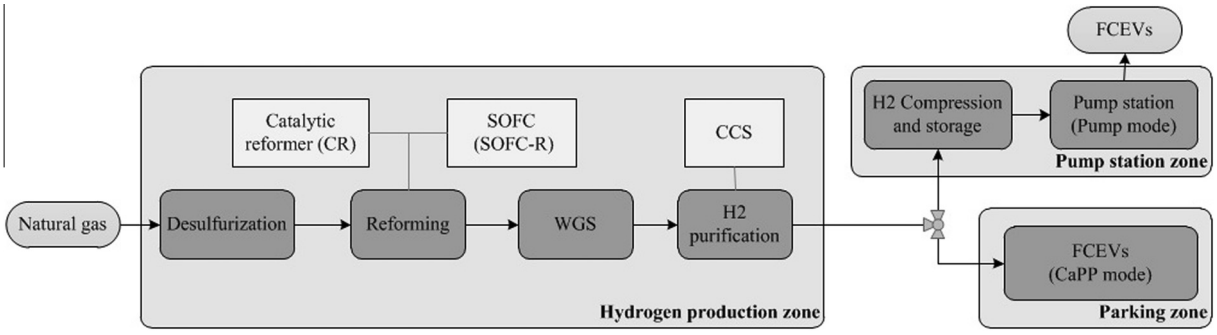

Fig. 2. Flow process of the hydrogen production plant; technology options assessed and product flows.

The evaluation is carried out in the two different operation modes of the facility:

- CaPP mode. It concerns the open period of the facility (10 h/day). The hydrogen produced (H_2 production zone) is directly supplied to the FCEVs (parking zone).
- Pump mode. It is related to the closed period of the facility (14 h/day). The hydrogen produced (H_2 production zone) is pumped and stored at 750 MPa (Pump station zone). It is further used in an external pump station to fill the fuel tank of both the parked FCEVs (when leaving the facility) and other FCEVs.

In addition, two auxiliary models are simulated to enable analysis of the four system designs per mode: FCEVs power system and hydrogen compression and storage unit. The FCEV power system is simulated to estimate the electricity and heat produced by the FCEVs either while parked (CaPP mode) or on the road (Pump mode) whereas the hydrogen compression and storage unit provides an estimation of the electricity consumption by the compressors and heat produced by the coolers.

2. Systems description

Each system design differs by (Fig. 2):

- Reforming unit: a catalytic reformer (CR) or a SOFC as a reformer (SOFCR).
- Option of integration of a CCS unit (in the hydrogen purification unit).

To clearly describe and explain the results of all four system designs, each one is identified by its abbreviation (Table 1).

2.1. Reforming technologies

Currently, hydrogen is mainly produced via natural gas steam reforming [37,38]. Hydrogen in petrochemical industry, is mainly used in the form of ammonia for fertilization and for methanol production [39].

2.1.1. Catalytic reformer

The reaction of methane with steam is moderately endothermic (Eq. (2.1)) and, therefore, an external heat source is required.

$$CH_4 + H_2O \rightarrow CO + 3H_2 \quad \Delta\bar{h}_0 = +206\ \text{kJ/mol} \tag{2.1}$$

In industry, typically, tubular-shaped reactors filled with a catalyst are employed for reforming natural gas [40–42]. The reforming process performed at a temperature higher than 923 K at high pressure (above 2 MPa). The most common catalyst used is a Ni-based catalyst due to present stability and low cost [41]. This catalyst is shaped into pellets to minimize the pressure loss and enhance heat transfer.

Table 1
System designs for the hydrogen production plant investigated in both operation modes.

Mode	System abbreviation	Reformer technology	CCS unit
CaPP	C-CR	Catalytic reformer	No
	C-CR/CCS	Catalytic reformer	Yes
	C-SOFCR	SOFC	No
	C-SOFCR/CCS	SOFC	Yes
Pump	P-CR	Catalytic reformer	No
	P-CR/CCS	Catalytic reformer	Yes
	P-SOFCR	SOFC	No
	P-SOFCR/CCS	SOFC	Yes

2.1.2. Solid oxide fuel cell

Solid oxide fuel cells (SOFC) are electrochemical devices with a capability of converting natural gas into electricity and heat. This feature is enabled by the high operating temperature and an appropriate catalyst such as Ni, commonly used in anode side and adequate to reform methane (80 mol% in natural gas) [43]. Consequently, the methane is converted into hydrogen and carbon monoxide in parallel with electrochemical oxidation [44]. Moreover, the reforming is also favored by the heat integration and usage of products formed in the electrochemical oxidation resulting in a simpler, more efficient, and compact system. Fan et al. reported that methane can be reformed internally without carbon deposition when appropriated steam content is supplied in common SOFC anode materials [45].

Nevertheless, the utilization of these devices as a reformer requires the minimization of the electrochemical oxidation. That is simply achieved by adjusting the fuel utilization to the point of balancing the heat required for the reforming reactions.

2.2. Gas processing

In a hydrogen production plant supplied by natural gas, gas processing units are essential to assure continuous operation, maximize production, and purify hydrogen.

2.2.1. Desulfurization

Traces of sulfur are often present in natural gas and act as poison to most of the catalysts and, therefore, need to be removed. A fix bed reactor using zinc oxide as a sorbent operating at 673 K has the capability of effectively removing all sulfur compounds in the stream [41,46]. The sorbent is regenerated by oxidizing zinc in a regeneration reactor.

2.2.2. Water gas shift

The reformed gas carries a significant amount of carbon monoxide that can be converted into hydrogen through the reaction with steam. Two adiabatic reactors in a series filled up with different catalysts are typically used: a high temperature reactor (583–723 K) filled with iron oxide-chromium oxide and a low temperature reactor (473–523 K) filled with copper oxide or zinc oxide [47,48]. Nevertheless, high temperature operation should be avoided to prevent catalyst degradation which can be accomplished by controlling the inlet temperature of the reformed gas. The percentage of unconverted carbon monoxide from the process ranges from 0.1% to 0.3% [49].

2.2.3. Pressure swing adsorption

In this simple process, the impurities are selectively adsorbed at very high pressure resulting in an outflow of high purity hydrogen. The purity level is defined by both the operational and purge pressures, gas composition and sorbents used.

The selection of an appropriate unit depends on the products desired. If only hydrogen is required, a Poly-bed PSA unit is frequently used and consists of several fixed bed reactors connected in parallel. A hydrogen recovery of 86% is achieved at approximately 2.1 MPa.

If carbon dioxide is also desired, a Gemini PSA unit is typically used which consists of two rows of several fixed bed reactors connected in a series. The first row allows the carbon dioxide capture (recovery of 94%) while, in the second row, high purity hydrogen (recovery of 87%) is obtained at 1.8 MPa.

From both technologies, the carbon dioxide and tail gas (purge gas) is obtained at environment pressure. The tail gas contains high calorific value which can be supplied to heat generators [41,50].

2.3. FCEVs

The main components of a polymer exchange membrane fuel cell (PEMFC) power system are a hydrogen tank, a water management, a PEMFC itself, and an air blower. These systems are usually coupled with batteries to provide extra power in the cycling operation. Composite high pressure hydrogen tanks are currently used in FCEVs due to its simple structure and easy charge–discharge operation [51]. These tanks have the capacity of storing more than 5 kg of hydrogen at 700 MPa permitting a driving range higher to 350 km [52,53].

3. Thermodynamic analysis

In this section, the numerical background used to calculate the efficiency of the several system designs is described. In addition, the assumptions that are made are listed.

3.1. Initial assumptions

In this thermodynamics analysis, these main assumptions are made:

- The hydrogen production plant and FCEVs power system reaches steady-state.
- Reference state is chosen as p_0 = 101.3 kPa and T_0 = 288.15 K.
- The average Groningen natural gas composition is used as a Refs. [54,55].
- The residence time and catalyst performance are sufficient to achieve chemical equilibrium reforming and water gas shift reactors.
- Electricity from the grid is assumed to be generated from natural gas power plants (main energy source for electricity production in Netherlands in 2012 [56]).
- Efficiency of electricity production and distribution by the electric grid in the Netherlands is estimated as 43% (LHV basis) and 96.2%, respectively [57,58].
- In the CCS option, a target of 85% of carbon capture is assumed (intermediate goal for RoadMap 2050 [1]).
- Pressure of 0.2 MPa from natural gas network is granted.
- Pressure drop in pump station is assumed 5 MPa.
- 100 cars are continuously parked during the open period of the facility. This is a random assumption in which it is expected that 5% of the university employees will own a FCEV in coming years.
- FCEVs are equipped with a 100 kW fuel cell system.
- 2500 kg/day of hydrogen are pumped in the external pump station.

3.2. Fuel cell calculations

All systems are simulated in a Cycle-Tempo software package [59]. It includes a fuel cell block and, consequently, is suitable for modeling fuel cell systems. A detailed description of fuel cell block calculations is available and can be consulted elsewhere [60–63].

3.3. Exergy calculations at unit level

To determine the main units causing major exergy destruction within the systems, an exergy analysis at unit level is performed. The exergy destroyed can be calculated through exergy balance:

$$\left(\sum_i \Phi_{\mathrm{mol},i}\cdot e_i\right)_{\mathrm{in}} - \left(\sum_i \Phi_{\mathrm{mol},i}\cdot e_i\right)_{\mathrm{out}} - \dot{W} - \dot{E}_{\mathrm{d}} = 0 \tag{3.1}$$

where Φ_{mol} and e are the mole flow and specific exergy of the inlet and outlet flows, $\dot{W}$ is the electric power, and $\dot{E}_{\mathrm{d}}$ is the exergy destruction in the unit. The specific exergy of a flow is given by the summation of both the physical and chemical specific exergies of the components in the mixture [64]:

$$e = \sum_i y_i\cdot\left(e_i^{\mathrm{PH}} + e_i^{\mathrm{CH}}\right) \tag{3.2}$$

whereby y is the mole fraction of the component ith in the mixture. The specific physical exergy is calculated by:

$$e_i^{\mathrm{PH}} = \left(\overline{h}_i - \overline{h}_{0,i}\right) - T_0\cdot\left(\overline{s}_i - \overline{s}_{0,i}\right) \tag{3.3}$$

This exergy corresponds to the variation of both the mole enthalpy ($\overline{h}$) and entropy ($\overline{s}$) of the component at its partial pressure (p_i) and temperature of the mixture to its partial pressure (p_j) and temperature in the mixture at reference conditions (p_0, T_0). The chemical exergy of the component is calculated by the summation of four different reversible work terms: (1) isothermal compression of the component to the standard pressure, (2) chemical conversion (isothermal reaction) of the component into an existing component in the environment at standard conditions (if required); (3) isothermal expansion of the existing component to its partial pressure in the environment; and (4) isothermal compression of the stoichiometric oxygen for the chemical conversion from its partial pressure in the environment to standard pressure. Nevertheless, for standard temperature and pressure conditions, the standard chemical exergy values of components (e_0^{CH}) can be obtained from tables (sum of terms 2, 3 & 4) [65]. Hence, the chemical exergy of the component is calculated as:

$$e_i^{\mathrm{CH}} = \overline{R}\cdot T_0\cdot\ln\left(\frac{p_j}{p_0}\right) + e_{0,i}^{\mathrm{CH}} \tag{3.4}$$

3.4. Exergy efficiencies

The exergy efficiency of every system design per operation mode is determined by the summation of the efficiency of each product obtained from the system. Then the results obtained are used to determine the facility efficiency (24 h operation basis) considering the system efficiency in both operation modes.

3.4.1. Products exergy efficiency

Concerning the electric exergy efficiency ($\varepsilon_{\mathrm{electric}}$), two cases are distinguished: excess and no electricity production within the system. For the first case, it is defined as:

$$\varepsilon_{\mathrm{electric}} = \frac{\dot{W}_{\mathrm{produced}} - \dot{W}_{\mathrm{aux}}}{\dot{E}_{\mathrm{NG}}} \tag{3.5}$$

whereby $\dot{W}_{\mathrm{produced}}$ is the electricity produced by the SOFCR and/or FCEVs parked, and $\dot{W}_{\mathrm{aux}}$ is the auxiliary components' electricity consumption. On the other hand, if no electricity is produced within the system, the case of both CR-based systems running in Pump mode, electricity from the grid is supplied. As a consequence, electricity is not considered as a product in these systems. Nevertheless, for a coherent comparison, an equivalent amount of natural gas ($\dot{E}_{\mathrm{NG,add}}$) corresponding to the primary energy required to produce the electricity by the electric grid is added to the inlet exergy of natural gas:

$$\dot{E}_{\mathrm{NG,add}} = \frac{\dot{W}_{\mathrm{aux}}}{\left(\eta_{\mathrm{production}}/f_{\mathrm{ex}}\right)\cdot\eta_{\mathrm{distribution}}} \tag{3.6}$$

in which $\eta_{\mathrm{production}}$ and $\eta_{\mathrm{distribution}}$ are the electric energy efficiency (LHV basis) of the electricity production and distribution in the

electric grid, and f_{ex} is the exergy factor of natural gas calculated by the ratio of the LHV and specific exergy. The value obtained from Eq. (3.6) is then added to the inlet exergy of the natural gas in the system to determine the heat and mobility exergy efficiencies for systems without internal electricity production.

The heat exergy efficiency is calculated by:

$$\varepsilon_{heat} = \frac{\dot{E}_Q}{\dot{E}_{NG}} \tag{3.7}$$

where $\dot{E}_Q$ is the heat exergy of the hot water generated in the system.

Mobility exergy efficiency is calculated by the multiplication of the exergy of the hydrogen (stored in the pump station) by the electric exergy efficiency ($\varepsilon_{electric,FCEVs}$) of the FCEV power system on the road. Consequently, it is calculated by:

$$\varepsilon_{mob} = \frac{\varepsilon_{H_2} \cdot \varepsilon_{electric,FCEVs}}{\dot{E}_{NG}} \tag{3.8}$$

3.4.2. Combined exergy efficiency

A combined efficiency of each product considering both CaPP and Pump modes is crucial to determine the most efficient system design. This efficiency is defined as:

$$\varepsilon_{comb,j} = \frac{\sum_{mode}\left(\Phi_{mol,H_2} \cdot \varepsilon_j \cdot \Delta Time\right)_{mode}}{\sum_{mode}\left(\Phi_{mol,H_2} \cdot \Delta Time\right)_{mode}} \tag{3.9}$$

where Φ_{mol,H_2} and $\Delta Time$ are the flow rate of hydrogen produced and hours per day in the respective operation mode, and ε is the exergy efficiency of each product j (electricity, heat and mobility). The total combined efficiency is then calculated by the summation of all combined efficiencies of all products.

4. System modeling

This section is split into three parts corresponding to the three zones of the facility. In the hydrogen production zone, the four different system designs are described whereas, in the parking zone and pump station zone, the auxiliary systems are described to perform the assessment of the system design in both the CaPP and Pump modes.

The input parameters for the reformer units and FCEV power system are listed in Table 2. The isentropic efficiency of the compressors is 0.75 [66], and the electromechanical efficiency of electromotors coupled with compressors and pumps is selected based on the standard IEC 60034-30 in category IE2 4-pole type for the range specified [67]. In case of devices with lower and higher rated power, the efficiency is fixed at 78% and 95.5%, respectively.

4.1. H_2 production zone

4.1.1. C-CR and P-CR

As illustrated in Fig. 3, the first step of the process employs a fixed bed reactor filled up with zinc oxide operating at 673 K to remove undesired sulfur compounds from natural gas at 2.2 MPa. After, the stream is reheated to 1073 K before entering the catalytic reformer unit to produce syngas. The heat required for the unit is generated by combustion tail gas from the PSA unit. In the next step, the syngas enters the WGS unit composed of two reactors connected in a series operating at different temperatures (623 K and 493 K) to convert carbon monoxide into hydrogen. The stream is then cooled to condensate the steam and sent to a Poly-bed PSA unit to produce pure hydrogen at 2.1 MPa and 298 K.

Table 2
Input parameters.

Catalytic reformer unit		
S/C ratio [68]	2.5	mol/mol
Reformer pressure [41]	0.45/2.2[a]	MPa
Reformer temperature [41]	1023	K
Burner outlet temperature	1573	K
Burner operating pressure	0.12	MPa
SOFCR unit		
S/C ratio [45]	2	mol/mol
Operating pressure	0.15	MPa
Operating temperature [62]	1123	K
Current density (maximum)	2500	A/m^2
Area specific resistance, R_{eq} [62]	0.5	$\Omega\,cm^2$
Oxidant utilization, U_{ox}	<0.65	mol/mol
FCEVs power system [69,70]		
Fuel cell pressure	0.15	MPa
Anode/cathode inlet temp.	353	K
Anode and cathode inlet RH	80	%
Net power (@ 25% load)[b]	2500	kW
Cell voltage	0.83	V
Current density	2750	A/m^2
Fuel utilization (per pass/total), U_f	0.67/0.98	mol/mol
Oxidant utilization, U_{ox}	0.55	mol/mol
Cool. water temp. (In/Out)	347/350	K
Isentropic efficiency blower, η_{is}	75	%
Power conditioner efficiency	97	%

[a] System design: with CCS/without CCS.
[b] Corresponding to 100 FCEVs.

The pure hydrogen is then redirected either to the parking zone (C-CR) and expanded to 0.17 MPa of the FCEV power system or to the pump station zone (P-CR).

The flue gas leaving the reformer is conducted to a heat recover steam generator (HRSG) unit and then used to produce heat and water in a heat exchanger and condenser before being exhausted to the environment.

4.1.2. C-CR/CCS and P-CR/CCS

Although high operation pressure reduces the methane conversion in the reformer unit, it favors the plant efficiency by avoiding a gaseous state compression of the syngas in a downstream stage. However, as it is shown in Fig. 3 (both additional and replaced components are highlighted), this system requires a 2-level pressure to reach the target of carbon capture. Therefore, the reforming occurs at an intermediate pressure (0.45 MPa) to promote higher methane conversion in the reformer and further, after the WGS unit, the pressure is increased to 1.8 MPa before entering the PSA unit. Consequently, this system is equipped with an additional compressor after WGS, and the Poly-bed PSA unit is replaced by a Gemini PSA unit to permit the recovery of carbon dioxide. Additionally, a 3-way valve is added after the Gemini PSA unit in order to supply sufficient energy to the burner. This is due to the low amount of energy of the tail gas from the PSA unit which resulted from the high conversion of methane in the reformer. The recovered carbon dioxide is then compressed in a double-stage compressor, liquefied with cold water, and stored for CO_2 pipeline transportation. Optimal inlet pressure can vary from 9 to 13 MPa, and in this study the worst scenario is chosen (13 MPa) [71]. As mentioned previously, the hydrogen is then diverted to the parking zone and expanded to 0.17 MPa (C-CR/CCS) or to the pump station zone (P-CR/CCS).

The flue gas leaving the reformer follows similar processing before being exhausted to the environment.

4.1.3. C-SOFCR and P-SOFCR

The flow process of these system designs is illustrated in Fig. 4. It is similar to the C-CR and P-CR system designs. However, in these

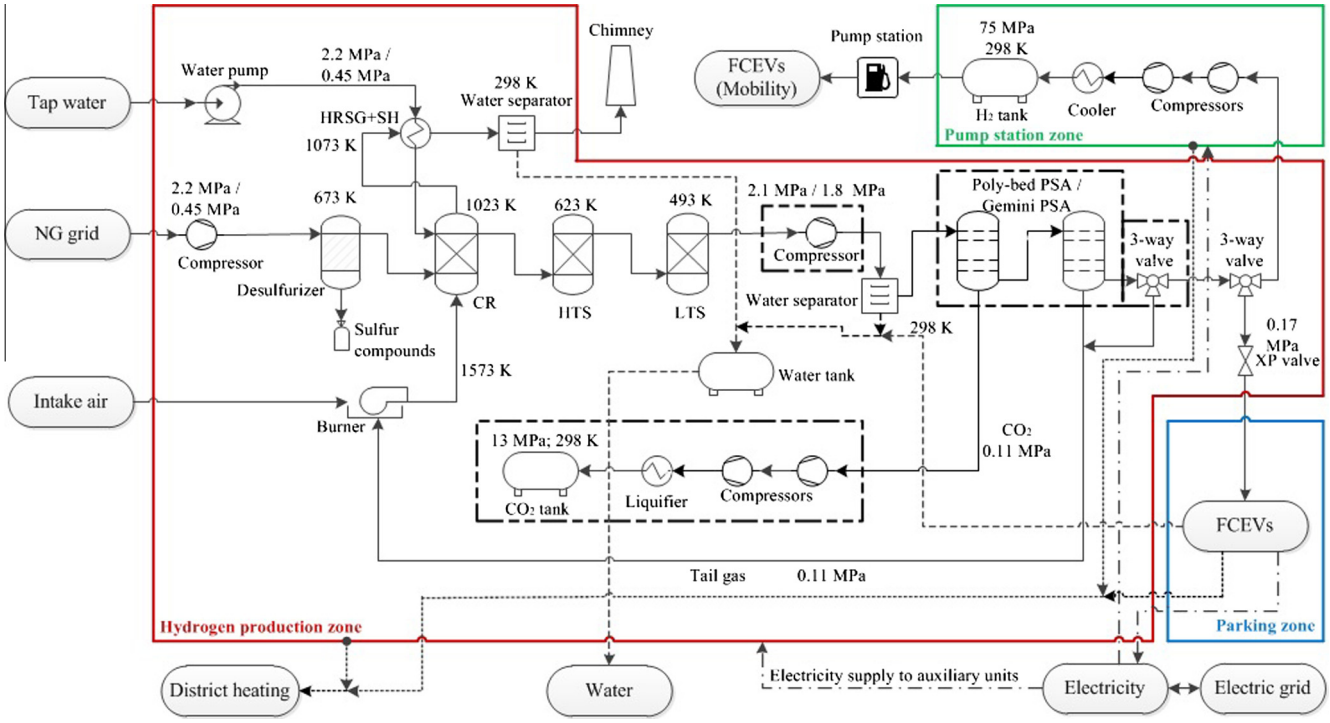

Fig. 3. Simplified flow process of the CR-based system designs: CaPP mode – H_2 is diverted to parking zone; Pump mode – H_2 diverted to pump station zone (hot water heat exchangers not shown).

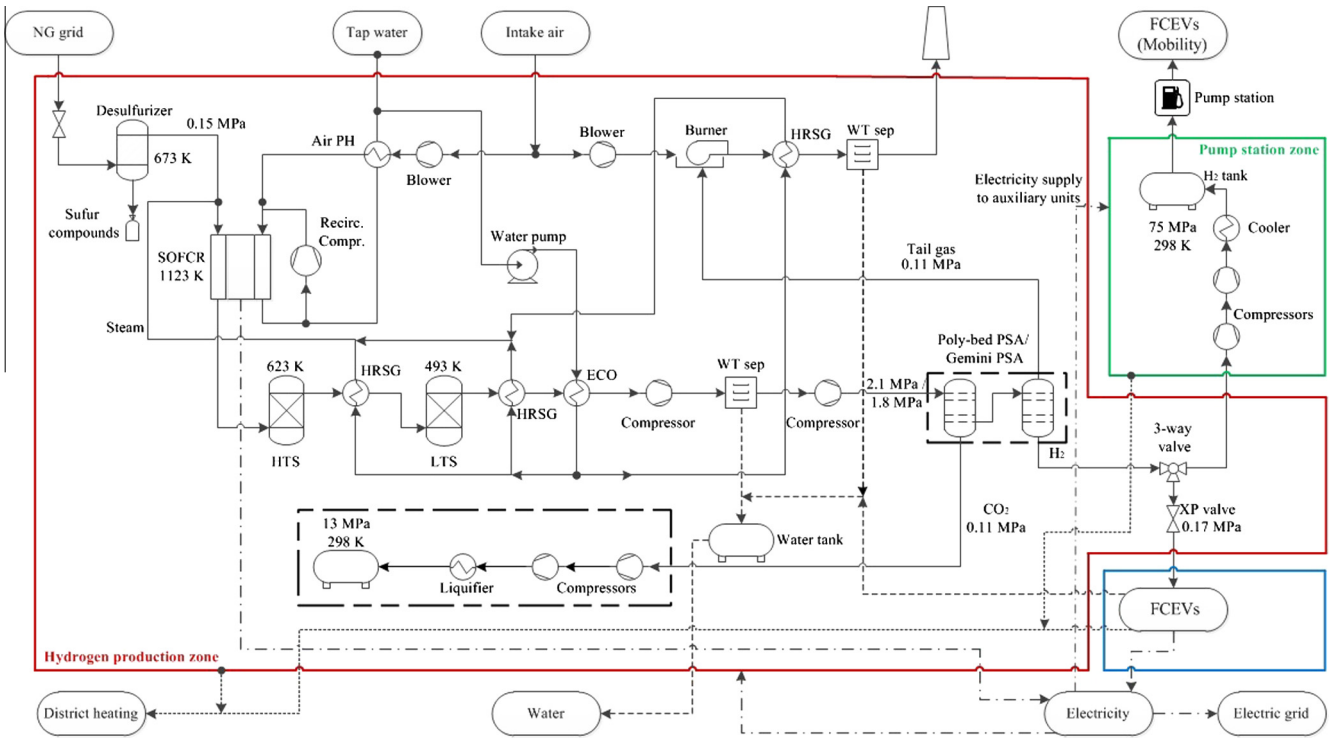

Fig. 4. Simplified flow process of SOFCR based system designs: CaPP mode – H_2 is diverted to parking zone; Pump mode – H_2 diverted to pump station zone (hot water heat exchangers not shown).

system designs, the catalytic reformer unit is replaced by an SOFC unit running as a reformer. As a consequence, operating at low pressure (0.15 MPa) is favored instead. High pressure would increase the power consumption of the SOFCR air blower, considerably reducing the efficiency of the system. Consequently, the rich-hydrogen stream needs to be pressurized (2.1 MPa) before entering the PSA unit. In addition, the tail gas purged by the PSA unit is burned to generate heat for a heat recovery steam generator (HRSG).

Concerning the SOFCR unit, it should be noted that equal active area is used in both CaPP and Pump modes. The maximum current

density specified in Table 2 is used to determine the SOFC active area for the greater hydrogen production demand (0.05 kg/s) by the unit (P-SOFCR). This SOFC active area is then used to simulate the other system design (C-SOFCR).

4.1.4. C-SOFC/CCS and P-SOFCR/CCS

The integration of a CCS unit requires minimal changes compared to the C-SOFCR and P-SOFCR system designs. For these system designs, the substitution of the Poly-bed PSA unit by the Gemini PSA unit and addition of compressors, liquifier, and tank units to compress and store the carbon dioxide are the different units and highlighted in Fig. 4. A similar principle is applied to determine the active area of the SOFCR unit. A simplified analysis and simulation of the CCS is done. The model design consists of a double-stage compressor with intercooler (338 K) and a liquifier using cold water as cooling medium. The carbon dioxide storage conditions are fixed at 13 MPa and 298 K which can be further used for other purposes.

4.2. Auxiliary models

4.2.1. Parking zone: FCEVs power system

The FCEVs power system is presented in Fig. 5. It represents a PEMFC power system, which is scaled up to the number of vehicles parked. This scaling up does not affect the efficiency, with exception for the cooling water pump (702) which pumps cooling water to all parked vehicles and is located in the facility.

In total, three connectors are available: low pressure hydrogen supply (102) and hot water (703,708) lines. The low pressure hydrogen stream is supplied by the hydrogen production plant and mixed with the unreacted hydrogen. It is then sent to the electric heater (104) and the humidifier to control the entering temperature and humidity in the PEMFC. Regarding the cathode stream, intake air (201) is compressed in an air blower and then exchanges water vapor and heat, in the membrane humidifier, with the outlet cathode flow. The membrane humidifier is represented by the apparatuses 202, 204, and 205 (dashed line zone). Extra water is supplied by a deposit tank (513). The liquid water that is produced and separated in liquid separators (107,206) is stored in the tank (401). The fuel cell system operation parameters are specified by the technical data of the current status for automotive applications and listed in Table 2 [69,72].

Finally, hot water is used to remove the heat generated in the fuel cell and stored in a hot water tank (701). Two 3-way valves (704,705) are used to deviate the water from the radiator (707) of the FCEV.

4.2.2. Pump station zone: hydrogen compression and storage unit

Figs. 3 and 4 show the compression configuration for the parking zone. A double-stage compressor with intercooler followed by

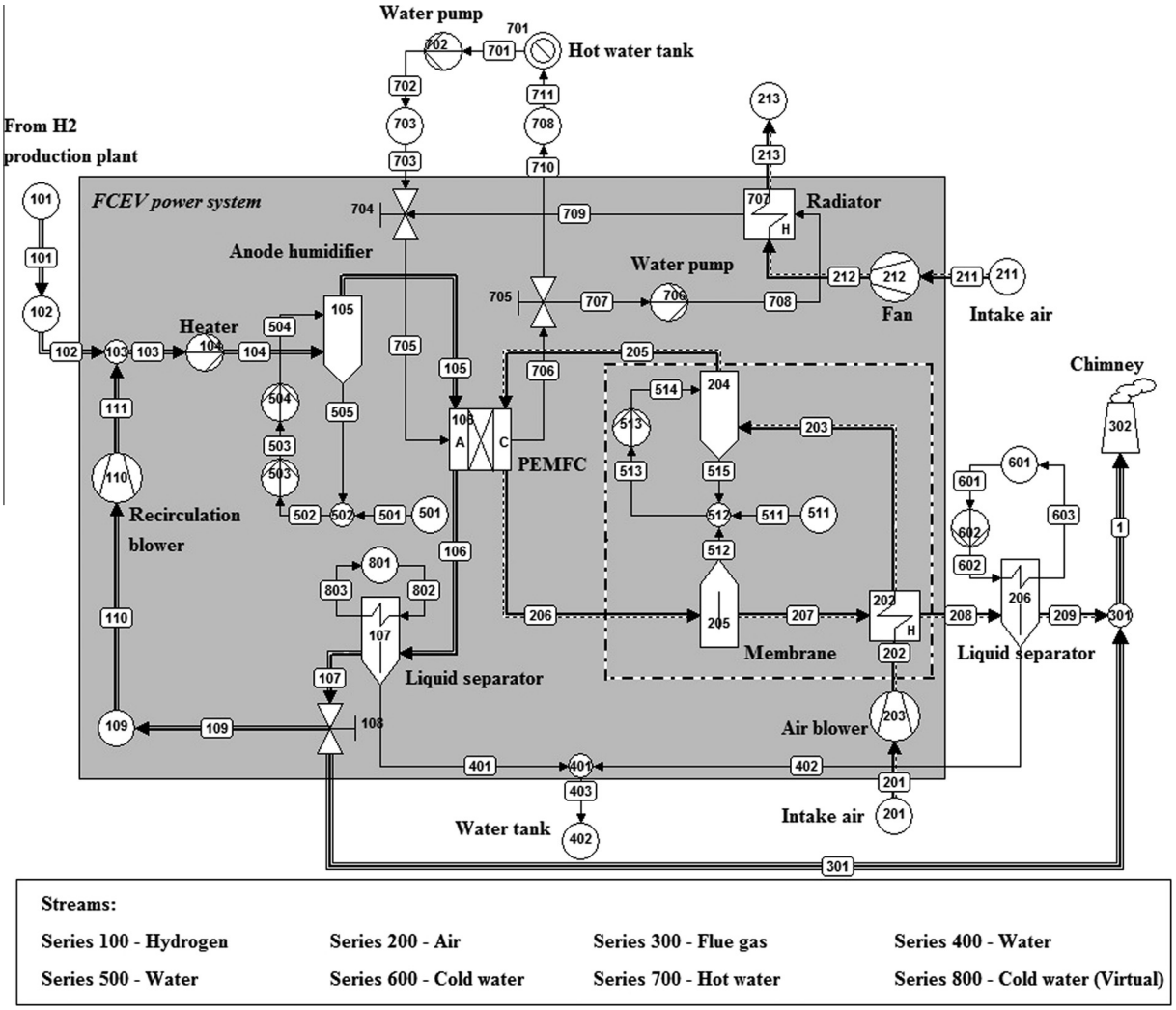

Fig. 5. FCEVs power system built in Cycle-Tempo [59].

a final cooling stage is used to compress the hydrogen to 75 MPa at 298 K. The outlet temperature of the hydrogen from the intercooler is fixed at 338 K.

5. Results and discussion

This section is split in 3 main parts. Firstly, the exergy analysis results obtained for all 4 system designs in each different operation mode are discussed, secondly, the combined efficiency and, finally, heat and water produced.

5.1. CaPP mode

The results obtained for the four system designs are depicted in Fig. 6 for the two products obtained: electricity and heat. Detailed values of the performance of all system designs are summarized in Table 3. In this mode, the hydrogen produced in the hydrogen production zone is supplied to the parking zone. By simulation of the FCEVs power system, a flow rate of the hydrogen to be produced is estimated at approximately 0.0356 kg/s representing an exergy flow of 4208 kW at 0.17 MPa and 298 K. This flow is then conducted to the parking zone to produce electricity (2500 kW, $\varepsilon_{electric,FCEV} = 59.4\%$) and heat (226 kW; $\varepsilon_{Q,FCEV} = 5.4\%$) in exergy. Since both electricity and heat produced in the parking zone are equal for all four system designs, the individual discussion of each system design is only focused on the hydrogen production subsystem (H_2 production zone). Further discussion is taken to compare results obtained from all system designs and, therefore, includes the results of both H_2 production and parking zones. In Table B.6 is listed the composition and flow rates of the main streams and in Table C.7 the operating parameters of the SOFCR units.

5.1.1. C-CR and C-CR/CCS vs. C-SOFCR and C-SOFCR/CCS

The aim of this study is primarily to evaluate the performance of the two different reforming units and the impact of these units in the system efficiency. As can be noted in Fig. 6 and Table 3, systems employing SOFCR units exhibit higher efficiency (63–65%) than CR-based systems (31–39%). This difference in efficiency results from three different aspects: (1) heat integration in the reforming unit; percentage ratio of the hydrogen exergy at outlet of the H_2 production zone (related to the total exergy output), and (3) the S/C required for the reforming unit. Regarding the reforming unit, the existing catalytic reformer causes threefold greater exergy destruction compared to the SOFCR unit. This mainly results from the different heat integration process in the unit. As shown in Fig. 3, the catalytic reformer is equipped with a burner to provide heat to the unit which results in a great exergy destruction, aspect very common in thermal processes. On the other hand, in the SOFCR unit, heat is generated by electrochemical oxidation of a certain amount of reformed products and, consequently, less exergy destroyed. However, this aspect also leads to an increase of natural gas consumption in the system. Moreover, the different reforming technology also influences the exergy percentage ratio of the products (related to the total exergy output) at the outlet of the hydrogen production zone. As observed, the exergy of hydrogen is approximately 92% of the total exergy output in the C-CR system design in contrast to approximately 40% in C-SOFCR system design. This fuel exergy is used for electricity and heat production in the FCEVs power system with an efficiency of approximately 63%. Consequently, the higher the percentage ratio of the hydrogen exergy, the lower the efficiency for the CaPP mode. Finally, SOFCR-based systems require a low S/C ratio which leads to a low amount of steam production and, consequently, smaller exergy destruction in heat exchangers.

It is also observed that, in CR-based systems, part of the electricity produced by the FCEVs needs to be supplied to the auxiliary units. Consequently, the net electricity produced is reduced. In contrary, SOFCR-based systems are capable of producing electricity within the H_2 production zone and, hence, the electricity produced by FCEVs is totally exported to the grid.

5.1.2. C-CR vs C-CR/CCS and C-SOFC vs C-SOFC/CCS

This comparison aims to evaluate the impact on the system efficiency by integration of a CCS unit. The results obtained in both CaPP and Pump modes exhibit similar trends as illustrated in Tables 3 and 4. Consequently, the discussion is only taken here.

As expected, the integration of a CCS unit reduces system efficiency. This reduction is more noticeable in CR-based system designs with a value up to 8% whereas, in SOFCR-based system designs, the reduction is lower at approximately 2%. All of this additional exergy destruction is shown in Figs. 6 and 7 by comparing the increment of exergy destruction in the reformer ($E_{d,CR}$ and $E_{d,SOFCR}$), the PSA unit ($E_{d,PSA}$ compared to $E_{d,PSA\&CCS}$), different compression configurations ($E_{d,others}$), and additional exergy loss of the outlet flow of carbon dioxide ($E_{loss,CO2}$). Concerning the CR-based system designs, additional entropy is generated due to four different factors: (1) higher methane conversion in the reforming unit which requires higher heat production in the burner; (2) requirement of compression of syngas instead of the compression of natural gas and liquid water in C-CR system design; (3) the entropy generation by the compressors and heat exchangers of the CCS unit; and (4) the increase in exergy loss by the CO_2 outflow. For the SOFCR-based system designs, the compressors and heat exchangers of the CCS unit contribute to additional entropy generation and the increase in exergy loss by CO_2 outflow are the two factors contributing to the reduction in efficiency.

5.2. Pump mode

A daily hydrogen production of 2500 kg is required for the external pump station results in a hydrogen production flow of 0.05 kg/s which is converted into 3716 kW ($\varepsilon_{electric,FCEV} = 59.5\%$) of mobility. The exergy flows are illustrated in Fig. 7 and the output exergy values are listed in Table 4 for the three products obtained: electricity, heat, and mobility. The latter product is estimated by the simulation of the FCEVs power system supplied by hydrogen at storage conditions (70 MPa; 298 K) and considering electricity as the only product. It is assumed that an average operation load of an FCEV on the road is 25%.

Regarding the pump station zone, the compression of the hydrogen to 75 MPa consumes 429 kW for system designs employing a Poly-bed PSA unit recovering 49 kW in heat exergy and 456 kW for system designs employing a Gemini PSA unit producing 53 kW in heat exergy.

Concerning the hydrogen production zone, all four system designs assessed here are similar to the ones assessed in the CaPP mode. As a result, similar operation parameters such as pressure, temperature, conversion efficiencies, hydrogen recovery, and flow compositions are obtained for the H_2 production zone. However, the demand in hydrogen production is higher and, therefore, higher flow rates of the inlet streams and subsequently higher electricity consumption by the auxiliary units are obtained. Therefore, only the difference in flow rates and energy consumed by the auxiliary systems are described for each system design. In Tables B.6 and C.7 are listed the composition and flow rates of the main streams and the operating parameters of the SOFCR units, respectively.

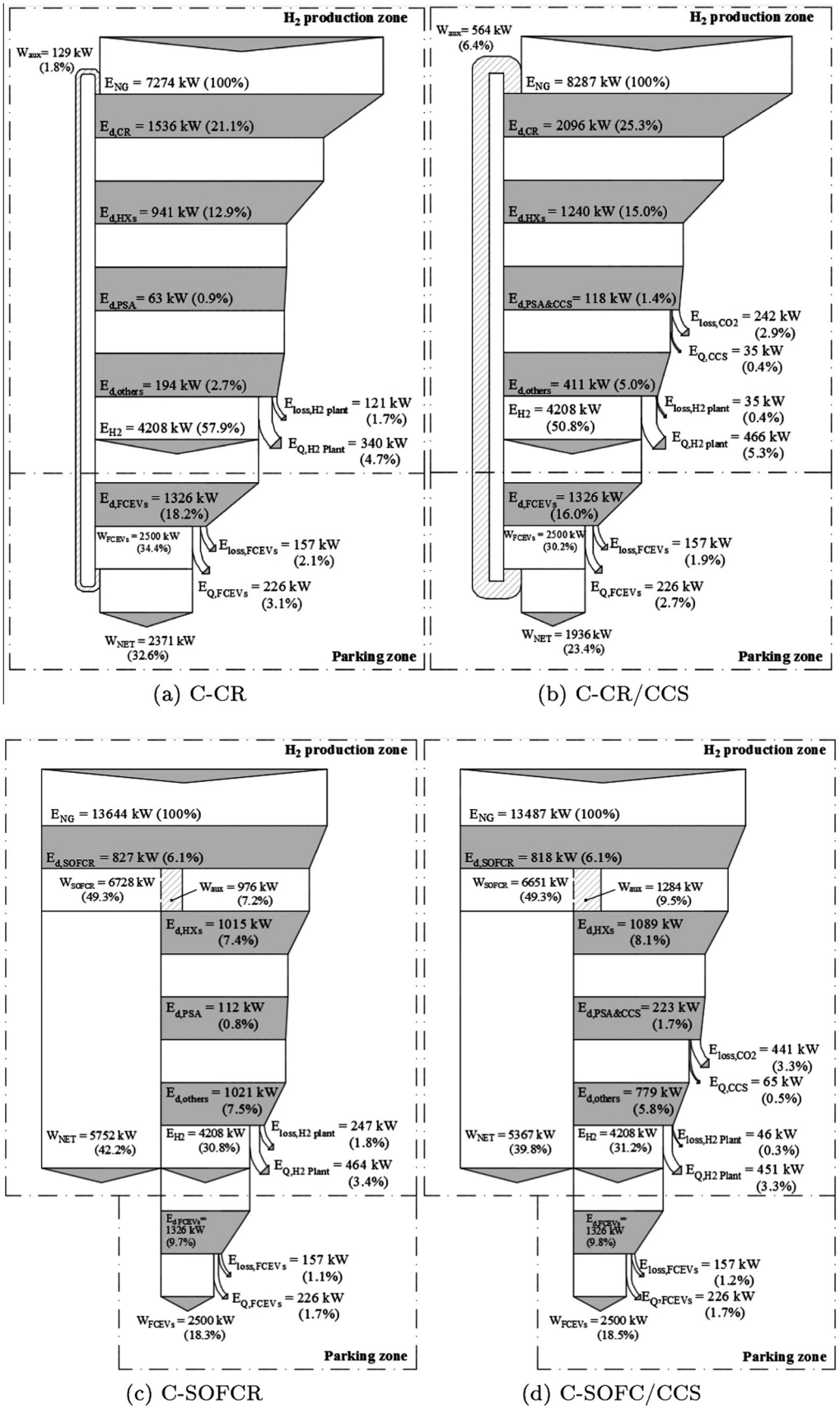

Fig. 6. Exergy flow diagrams of the four system designs in CaPP mode.

Table 3
Exergy flows and efficiencies of products of all 4 system designs in CaPP mode.

	Product	C-CR		C-CR/CCS		C-SOFCR		C-SOFCR/CCS	
		(kW)	(%)	(kW)	(%)	(kW)	(%)	(kW)	(%)
	Natural gas	7274	100.0	8287	100.0	13644	100.0	13487	100.0
H_2 production zone	$\dot{W}_{SOFCR}$					6728	49.3	6651	49.3
	$\dot{W}_{aux}$	−129		−494		−976		−1284	
	Heat	340	4.7	501	5.7	464	3.4	516	3.8
	Hydrogen	4208	57.9	4208	50.8	4208	30.8	4208	31.2
Parking zone	$\dot{W}_{FCEVs}$	2500	34.4	2500	30.2	2500	18.3	2500	18.5
	Heat	226	3.1	226	2.7	226	1.7	226	1.7
CaPP mode	$\dot{W}_{Net}$	2371	32.6	1936	23.4	8252	60.5	7867	58.3
	Heat	566	7.8	727	8.4	690	5.1	732	5.5
	Total	2937	40.4	2663	31.8	8942	65.6	8599	63.8

Table 4
Exergy flows and efficiencies of products of all 4 system designs in Pump mode.

	Product	P-CR		P-CR/CCS		P-SOFCR		P-SOFCR/CCS	
		(kW)	(%)	(kW)	(%)	kW	(%)	kW	(%)
H_2 production zone	Natural gas	10211	87.4	11633	80.0	17903	100.0	17697	100.0
	NG added[a]	1474	12.6	2892	20.0	–	–	–	–
	$\dot{W}_{SOFC}$					8369	46.7	8273	46.7
	$\dot{W}aux$	−181		−740		−1329		−1738	
	Heat	477	4.1	654	4.5	615	3.4	683	3.9
	Hydrogen	6056	51.8	6046	41.7	6056	33.6	6046	34.2
Pump station zone	Electricity	−429		−456		−429		−456	
	Heat	49	0.4	53	0.4	49	0.3	53	0.3
	Hydrogen	6240	53.4	6240	43.0	6240	34.9	6240	35.3
FCEVs on road	Mobility	3716	31.8	3716	25.6	3716	20.8	3716	21.0
Pump mode	Electricity					6611	36.9	6079	34.5
	Heat	526	4.5	707	4.9	664	3.7	736	4.2
	Mobility	3716	31.8	3176	25.6	3716	20.8	3716	21.0
	Total	4242	36.3	3883	30.5	10451	61.4	10299	59.7

[a] Equivalent flow of natural gas required to produce the electricity for the auxiliaries in a Natural gas power plant.

5.2.1. P-CR and P-CR/CCS vs. P-SOFCR and P-SOFCR/CCS

Similarly to the CaPP mode, it can be noted that the catalytic reformer is the main unit causing exergy destruction in the P-CR system design. The exergy destruction in this component is still threefold compared to the SOFCR unit. Another factor contributing to the low efficiency of this system is the inability to produce electricity internally. For reasonable comparison, we assumed that electricity should be produced from similar energy source. Therefore, an equivalent natural gas inlet flow is defined as input, representative of the primary energy required to produce electricity by the electric grid. From this flow, more than 50% is destroyed representing 5.2% and 7.4% of the exergy destruction in the system.

Regarding the output exergies from the system, it is observed that higher mobility efficiency is achieved in catalytic reformer-based systems. In the most efficient system design, an efficiency of 29% is obtained while, in SOFCR-based systems, 19% is determined. However, the total efficiency (33.6%) of the CR-based system design is unattractive for its implementation. This low efficiency results from the nature of the system, which has only mobility and heat as the output flows. Therefore, this low efficiency results from the combination of the high percentage ratio of the hydrogen exergy in the total exergy output from the hydrogen production plant which is reduced by the FCEVs efficiency, the low efficiency of electricity supplied by the grid, and the exergy destruction in the reforming unit. On the other hand, SOFCR-based systems exhibit a total efficiency of approximately 60%, almost twofold compared to catalytic reformer-based systems.

5.3. Combined exergy efficiency

In Fig. 8, the efficiency results of the combination of both CaPP and Pump modes are depicted.

As expected, in SOFCR-based systems, higher efficiency (61–63%) is obtained compared to catalytic-based reformer systems (31–38%). In SOFCR-based systems, the electricity efficiency has the highest value of all products and ranges from 42.5% to 45%, followed by the mobility efficiency (14%) and, finally, the heat efficiency of approximately 4–4.5%. On the other hand, catalytic reformer-based systems have mobility efficiency as the highest value of 17–21%, followed by electric efficiency (8–11%) and, finally, heat efficiency of 5.5–6%.

5.4. Other products

Although the main products desired from the facility are electricity and hydrogen, other products are produced and useful for other applications such as hot water to be used in a district heating network, and water are the products considered.

5.4.1. District heating

In Fig. 9 shows the heat production per day (hot water at 353 K) which includes both CaPP and Pump modes. In general, the heat production capacity is comparable for all system designs (100–110 MW h/day) with exception for the CR (combination of C-CR/P-CR) system design (83 MW h/day). The major contributor is the H_2 production zone representing 75–82% (26–29% in CaPP

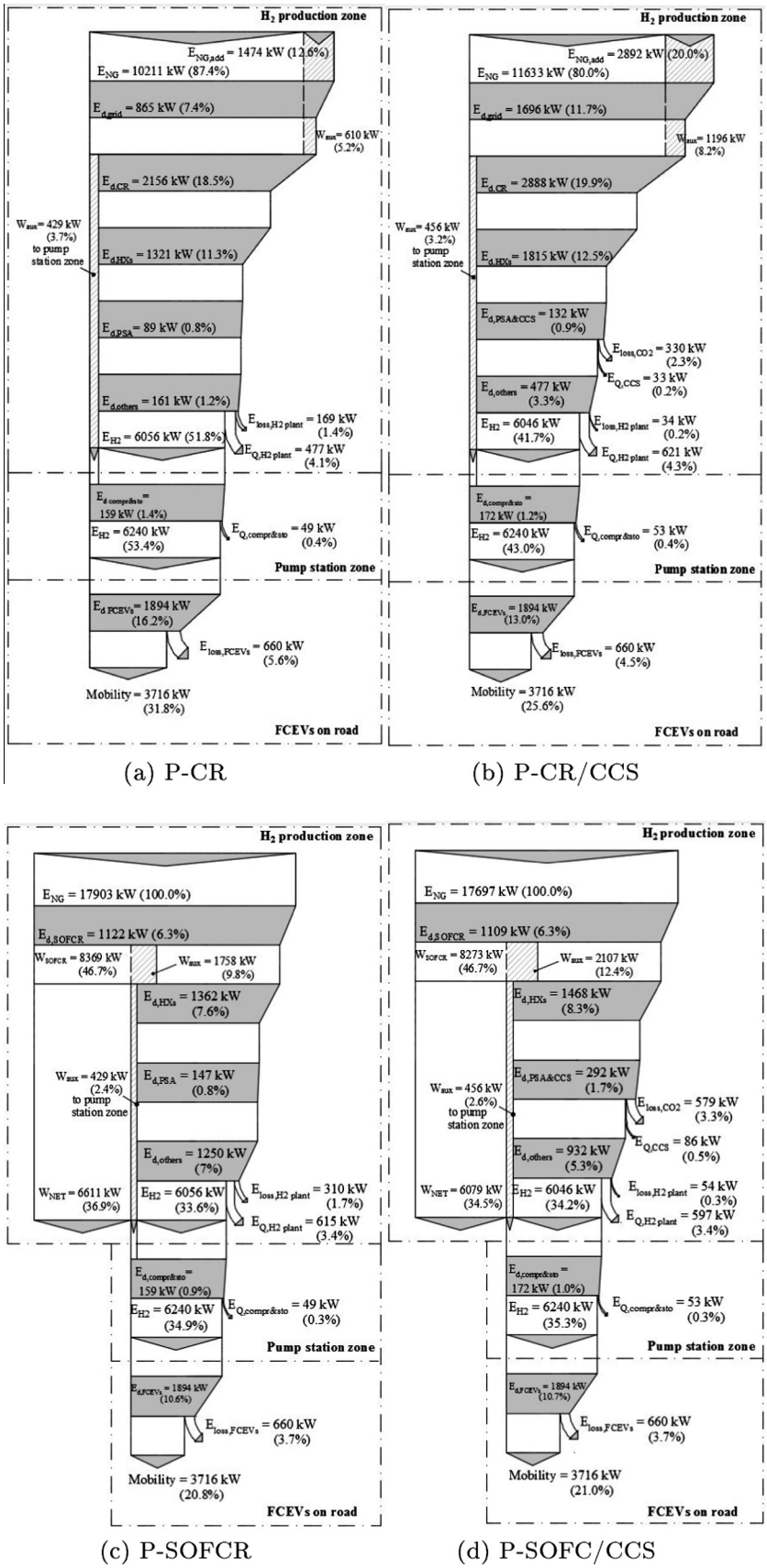

Fig. 7. Exergy flow diagrams of the four system designs in Pump mode.

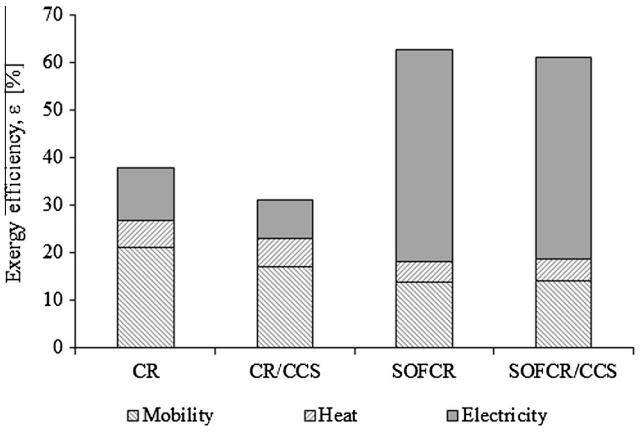

Fig. 8. Combined efficiency of all 4 system designs.

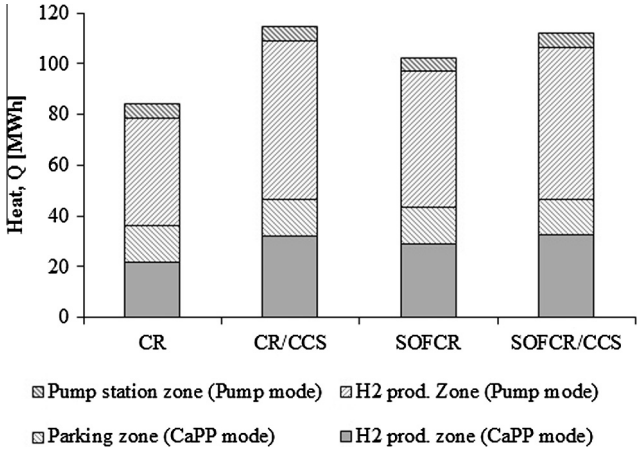

Fig. 9. Heat production capacity per day.

mode) of the total heat production capacity. The FCEVs (parking zone) contribute with 12–17% whereas the hydrogen compression and storage unit (pump station zone) modestly contributes with 5–6% of the total heat production.

5.4.2. Water

The water produced by every system design is depicted in Table 5. It can be observed that SOFCR-based system designs produce about 1.5 times as much water as the CR-based system designs. It results, as the balance shows, from the capability of water production by SOFC-based system designs. In CR-based system designs, 7–11 m^3/day are produced internally which determines that the FCEVs are the main water producer. In SOFCR-based system designs, 30% of the total water is produced by the FCEVs and the remaining by the SOFCR unit due to the electrochemical oxidation of a certain amount of reforming products. However, water produced in these systems may be contaminated with chromium and, consequently, not safe for potable use. Some studies have revealed that chromium in inter-connectors vaporizes and deposits in surfaces of electrodes contributing for major degradation in SOFCs [73,74]. New coatings are being developed to reduce the vaporization of this element, however, not capable to avoid completely [75]. Therefore it is also expected this element in the outlet anode stream.

Table 5
Water consumed and produced by each system design (m^3/day).

	CR	CR/CCS	SOFCR	SOFCR/CCS
Tap water	−49.1	−55.7	−64.3	−63.0
Produced	56.5	66.7	94.5	92.9
Balance	7.4	11.0	30.2	29.9

6. Conclusions

An assessment of the four different system designs for a novel concept of a parking lot for FCEVs used as power plant is carried out. Systems are distinct by the reforming technology unit and the option of having a CCS unit integrated. Through various thermodynamic simulations, the results reveal different advantages and disadvantages of the various options which are highlighted here:

- Solid oxide fuel cells as reformers significantly reduce exergy destruction when compared to the existing catalytic reformers. These units benefit of more efficient heat generation and low steam requirement. These factors significantly reduces entropy generation in the reformer and heat recovery steam generator units.
- SOFCR-based systems have the capability of producing of electricity at higher efficiency than the power plants feedinf the present day electric grid. Electricity from the electric grid (The Netherlands) is mostly produced by natural gas power plants with an average electrical efficiency of 43%.
- In SOFCR-based systems, almost twice as much natural gas is consumed for an equal amount of hydrogen production. The high efficiency electricity production in SOFCs reduces the amount of heat generated in electrochemical reactions. Therefore, high fuel utilization (vary from 66% to 69%) is required to provide heat for the reforming reactions.
- The reduction in efficiency by the integration of a CCS unit is significantly lower in SOFCR-based systems. This is due to changes in the system designs (PSA unit, additional CO_2 compressors and CO_2 liquefier). In contrast, for CR-based systems, the pressure of the reformer unit is reduced to achieve higher methane conversion. Therefore, an additional unit is employed (syngas compressor) and higher heat generation by the burner is required.
- Heat production capacity is comparable in almost all system designs. Nevertheless, it is also concluded that heat production per unit of input energy is higher in CR-based subsystems.
- Larger amounts of water can be produced in SOFCR-based systems. This is a result of higher fuel consumption for equal amount of hydrogen production.
- Mobility efficiency is higher for CR based-systems, however total efficiency is very low and, therefore, they are not very attractive. This is a result of the nature of the system, which is more directed for hydrogen production whereas SOFCR-based systems are targeted for both hydrogen and electricity production. In addition, the electricity consumed by auxiliary units is imported from the grid which is produced at lower efficiency.
- A trigeneration exergy efficiency (mobility, electricity and heat) of approximately 60% is achieved in SOFCR-based systems.

Acknowledgments

The Portuguese Foundation for the Science and Technology (FCT) is thanked for the financial support (Grant – SFRH/BD/77042/2011). This study is part of preliminary assessment of different system designs for the hydrogen production plant of the

CaPP infrastructure included in "The Green Village" project run by the Delft University of Technology in partnership with private companies.

Appendix A. The Green Village: "Our Car as Power Plant concept

The change to a clean and sustainable transport and energy sector is inevitable and ongoing. "The Green Village" programme through a series of clean, efficient and sustainable planned infrastructures intents to create, develop and demonstrate a sustainable environment in terms of integrity, flexibility and reliability for the energy and transportation sector [76]. The programme has already started as a platform. The entire programme is divided in three component lines: fuel cell electric vehicles prototypes to provide vehicle-to-grid services, hydrogen production, and smart grids/system integration.

"Car Park Power Plant" is the infrastructure focused on this study (Fig. A.10). It is a part of the integral innovation programme "Our Car as Power Plant" which consists of a parking garage integrated with an hydrogen production plant which enables fuel cell electric vehicles to produce power to be exported to the grid (vehicle-to-grid services). In addition, this concept also integrates a hydrogen pump station. The main objective of this plant is to create a flexible, clean and reliable power system that in the near future can compete and replace the existing fossil fuel based plants. The main aspects boosting this concept are described in the introduction of this paper.

In preliminary estimations, it is believed that the electricity production by this type of plant could achieve better electric efficiencies than conventional coal plants (38%) in full load capacity. Moreover, this new power unit has the advantage of achieving higher electric efficiencies in part-load operation in contrary to coal plants. This is crucial in our times due to the fluctuating power demand nature of the electric grid caused by the seasonality and fluctuating production capacity of the renewable energies as well as by the variable power consumption by consumers [34].

A.1. Progress status

As aforementioned, the programme consists of three component lines. In the first one, four prototype vehicles (two passenger cars, a bus, and a scooter) are being adapted or built by a partner company Accenda BV [77]. The first one (Fig. A.11a) is already adapted and capable to deliver power up to 10 kW. In the second line, an SOFC co-generation pilot plant is planned and is being developed for very high efficiency production of hydrogen and power. In the third programme line, a prototype electric connection for the FCEV to a very high efficient house located in our campus (Fig. A.11b) is being designed, and will become operational in April 2016. These three components will be used to test and improve the models and theory in the paper.

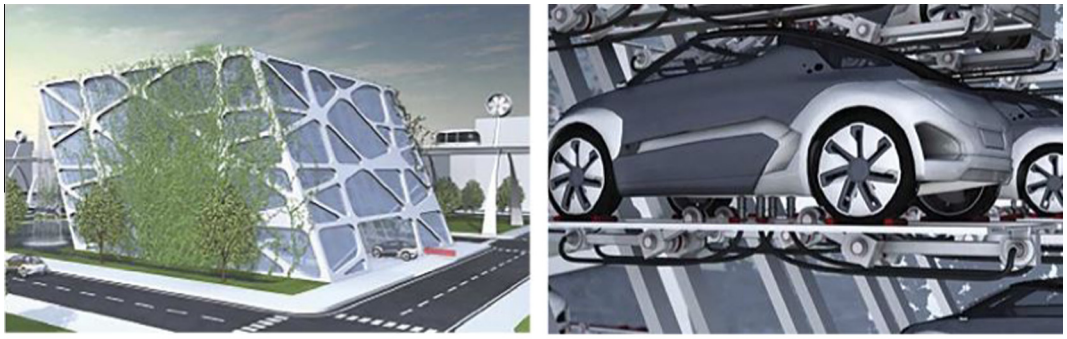

(a) CaPP facility concept (b) Schematic of connection of FCEVs

Fig. A.10. Planned Car as Power Plant infrastructure [34].

(a) Hyundai ix35 FCV [34] (b) Prt--Loger Decathlon House [78]

Fig. A.11. FCEV and house to be connected in the third programme line. (See above-mentioned references for further information.)

Appendix B. Flow composition of the system designs

Table B.6
Flow rates and composition of systems designs of the main streams.

Stream	Component	Units	CR	CR/CCS	SOFCR	SOFCR/CCS
NG	CH_4	mol%	81.3			
	C_3, C_4, C_5, C_6	mol%	3.5			
	CO_2	mol%	0.9			
	N_2	mol%	14.3			
	CaPP flow	kg/s	0.184	0.21	0.346	0.342
	Pump flow	kg/s	0.259	0.295	0.454	0.448
Steam	CaPP Flow	kg/s	0.46	0.52	0.62	0.62
	Pump flow	kg/s	0.62	0.73	0.82	0.81
Air cathode	CaPP flow	kg/s	–	–	4.23	4.18
	Pump flow	kg/s	–	–	5.86	5.77
After reforming	CH_4	mol%	7.8	1.9	0	0
	H_2	mol%	39.7	51.7	18.9	18.9
	CO	mol%	5.2	9.1	5.0	5.0
	H_2O	mol%	37.9	28.2	58.7	58.7
	CO_2	mol%	6.4	6.5	14.4	14.4
	N_2	mol%	3.0	2.7	3.0	3.0
After WGS	CH_4	mol%	7.8	1.9	0	0
	H_2	mol%	44.8	60.4	23.9	23.9
	CO	mol%	0.1	0.3	<0.1	<0.1
	H_2O	mol%	33.4	19.4	53.7	53.7
	CO_2	mol%	10.9	2.5	19.4	19.4
	N_2	mol%	3.0	2.7	3.0	3.0
Tail gas	CH_4	mol%	27.0	5.1	0	0
	H_2	mol%	21.7	83.5	12.9	41.7
	CO	mol%	0.2	0.9	0.2	0.8
	CO_2	mol%	40.0	2.5	74.9	15.6
	N_2	mol%	10.6	7.6	11.8	41.1
	CaPP flow	kg/s	0.337	0.127	0.815	0.124
	Pump flow	kg/s	0.473	0.179	1.07	0.163
H_2 to parking zone		kg/s	0.0356			
H_2 to pump zone		kg/s	0.05			

Appendix C. Operation parameters of the SOFCR units

Table C.7
SOFC operating parameters results.

Parameter	C-SOFCR	C-SOFCR/CCS	P-SOFCR	P-SOFCR/CCS
Cell voltage, V_{cell} (V)	0.803		0.786	
Current density, j (A/m^2)	1970		2500	
Fuel utilization, U_f	0.685		0.663	
Oxidant utilization, U_{ox}	0.6		0.534	
Cathode recirc. fraction	0.4		0.43	
SOFC active area	4390	4340	4390	4340
$\dot{W}_{SOFCR}$	6728	6651	8369	8273
ε_{SOFCR}[a] (%)	89.1	89.0	88.5	88.5

[a] Ratio of power produced by the exergy variation of both anode and cathode inlet and outlet flows of SOFCR.

References

[1] European Commission. A roadmap for moving to a competitive low carbon economy in 2050. COM. 112 final; 2011. <http://ec.europa.eu/clima/policies/roadmap/>.
[2] European Commission. Energy markets in the European Union in 2011; 2011. <http://ec.europa.eu/energy/gaselectricity/doc/>.
[3] European Commission. A portfolio of power-trains for Europe: a fact-based analysis. The role of battery electric vehicles, plug-in hybrids and fuel cell electric vehicles; 2012. <http://ec.europa.eu/research/fch/pdf/>.
[4] Pasaoglu G, Fiorello D, Martino A, Zani L, Zubaryeva A, Thiel C. Travel patterns and the potential use of electric cars – results from a direct survey in six European countries. Technol Forecast Soc Change 2014;87(0):51–9.
[5] Satyapal Sunita, Petrovic John, Read Carole, Thomas George, Ordaz Grace. The U.S. Department of Energy's National Hydrogen Storage Project: progress towards meeting hydrogen-powered vehicle requirements. Catal Today 2007;120(34):246–56. Proceedings of the Korea Conference on Innovative Science and Technology (KCIST-2005): Frontiers in Hydrogen Storage Materials and Technology.
[6] Evo. The drill of driving. Hyundai ix35 fuel cell arrives in UK; October 2014.
[7] Jason Inofuentes. Toyota announces FCV, a commercially viable fuel cell vehicle; January 2014.
[8] Nissan, Daimler and Ford Forge Fuel Cell Electric Vehicle Pact; January 2013.
[9] H2 infrastructure. A network of filling stations for Germany. CEP Energy Partnership; 2016.
[10] Takahashi Y, Kawagoe J. Nihon no Nenryou Denchi Jidousha no Hanbai Daisuu Yosoku (Sales forecast of fuel cell vehicles in Japan); 2014.
[11] Eurostat. Time spent, participation time and participation rate in the main activity by sex and age group – collection round 2000; April 2014. <http://epp.eurostat.ec.europa.eu/>.
[12] Wendel Cox. The transportation politics to envy – the US & Europe; March 2011.
[13] Mwasilu Francis, Justo Jackson John, Kim Eun-Kyung, Do Ton Duc, Jung Jin-Woo. Electric vehicles and smart grid interaction: a review on vehicle to grid and renewable energy sources integration. Renew Sustain Energy Rev 2014;34:501–16.
[14] Schill Wolf-Peter, Gerbaulet Clemens. Power system impacts of electric vehicles in Germany: Charging with coal or renewables? Appl Energy 2015;156:185–96.
[15] Donateo T, Licci F, Elia AD, Colangelo G, Laforgia D, Ciancarelli F. Evaluation of emissions of CO_2 and air pollutants from electric vehicles in italian cities. Appl Energy 2015;157:675–87.
[16] Neaimeh Myriam, Wardle Robin, Jenkins Andrew M, Yi Jialiang, Hill Graeme, Lyons Padraig F, et al. A probabilistic approach to combining smart meter and electric vehicle charging data to investigate distribution network impacts. Appl Energy 2015;157:688–98.

[17] Bishop Justin DK, Axon Colin J, Bonilla David, Tran Martino, Banister David, McCulloch Malcolm D. Evaluating the impact of V2G services on the degradation of batteries in PHEV and EV. Appl Energy 2013;111 (November):206–18.
[18] Marongiu Andrea, Roscher Marco, Sauer Dirk Uwe. Influence of the vehicle-to-grid strategy on the aging behavior of lithium battery electric vehicles. Appl Energy 2015;137:899–912.
[19] Hidrue Michael K, Parsons George R. Is there a near-term market for vehicle-to-grid electric vehicles? Appl Energy 2015;151:67–76.
[20] Noori Mehdi, Zhao Yang, Onat Nuri C, Gardner Stephanie, Tatari Omer. Light-duty electric vehicles to improve the integrity of the electricity grid through vehicle-to-grid technology: analysis of regional net revenue and emissions savings. Appl Energy 2016;168:146–58.
[21] Zhao Yang, Noori Mehdi, Tatari Omer. Vehicle to grid regulation services of electric delivery trucks: economic and environmental benefit analysis. Appl Energy 2016;170:161–75.
[22] Juul Nina, Meibom Peter. Road transport and power system scenarios for Northern Europe in 2030. Appl Energy 2012;92:573–82.
[23] Briguglio N, Ferraro M, Brunaccini G, Antonucci V. Evaluation of a low temperature fuel cell system for residential CHP. Int J Hydrogen Energy 2011;36(13):8023–9 [Hysydays].
[24] Gandiglio M, Lanzini A, Santarelli M, Leone P. Design and optimization of a proton exchange membrane fuel cell CHP system for residential use. Energy Build 2014;69(0):381–93.
[25] Gencoglu Muhsin Tunay, Ural Zehra. Design of a PEM fuel cell system for residential application. Int J Hydrogen Energy 2009;34(12):5242–8.
[26] Sammes NM, Boersma R. Small-scale fuel cells for residential applications. J Power Sources 2000;86(12):98–110.
[27] Kempton Willet, Tomic Jasna, Letendre Steven, Brooks Alec, Lipman Timothy. Vehicle-to-grid power: battery, hybrid, and fuel cell vehicles as resource for distributed electric power in California. California Air Resources Board and the California Environmental Protection Agency, and the Los Angeles Department of Water and Power, Electric Tansportation Program; 2001.
[28] Colmenar-Santos Antonio, Reino-Rio Cipriano, Borge-Diez David, Collado-Fernandez Eduardo. Distributed generation: a review of factors that can contribute most to achieve a scenario of DG units embedded in the new distribution networks. Renew Sustain Energy Rev 2016;59:1130–48.
[29] Colella Whitney, Rankin Aerel, Margalef Pere, Sun Amy, Brouwer Jack. Thermodynamic, economic, and environmental modeling of hydrogen (H2) co-production integrated with stationary fuel cell systems (FCS); November 2009.
[30] Hemmes K, Kamp LM, Vernay ABH, de Werk G. A multi-source multi-product internal reforming fuel cell energy system as a stepping stone in the transition towards a more sustainable energy and transport sector. Int J Hydrogen Energy 2011;36(16):10221–7 [European fuel cell 2009].
[31] Hemmes K, Zachariah-Wolf JL, Geidl M, Andersson G. Towards multi-source multi-product energy systems. Int J Hydrogen Energy 2007;32(10–11):1332–8 [EHEC2005].
[32] Yu Mengjing, Muy Suzann, Quader Farah, Bonifacio Abigail, Varghese Roshni, Clerigo Elisha, et al. Combined hydrogen, heat and power (CHHP) pilot plant design. Int J Hydrogen Energy 2013;38(12):4881–8.
[33] Hamad Tarek A, Agll Abdulhakim A, Hamad Yousif M, Bapat Sushrut, Thomas Mathew, Martin Kevin B, et al. Hydrogen recovery, cleaning, compression, storage, dispensing, distribution system and end-uses on the university campus from combined heat, hydrogen and power system. Int J Hydrogen Energy 2014;39(2):647–53.
[34] van Wijk Ad, Verhoef Leendert. Our Car as Power Plant. IOS Press BV; 2014. ISBN 978-1-61499-377-3.
[35] Breeze Paul. Natural gas-fired gas turbines and combined cycle power plants. In: Breeze Paul, editor. Power generation technologies. Boston: Newnes; 2014. p. 67–91 [chapter 4].
[36] Poullikkas Andreas. An overview of current and future sustainable gas turbine technologies. Renew Sustain Energy Rev 2005;9(5):409–43.
[37] Olateju Babatunde, Monds Joshua, Kumar Amit. Large scale hydrogen production from wind energy for the upgrading of bitumen from oil sands. Appl Energy 2014;118(0):48–56.
[38] Thompson Levi, Barbier Françoise, Burns Lawrence, Friedland Robert, Kikzer Edward, Nozic Arthur, et al. Report of the hydrogen production expert panel: a subcommittee of the hydrogen & fuel cell technical advisory committee. Technical report. United States Department of Energy; 2013.
[39] Abbas Hazzim F, Wan Daud WMA. Hydrogen production by methane decomposition: a review. Int J Hydrogen Energy 2010;35:1160–90.
[40] Rostrup-Nielsen JR. Steam reforming and chemical recuperation. Catal Today 2009;145:72–5.
[41] Liu Ke, Song Chunchan, Subramany Velu. Hydrogen and syngas production and purification technologies. John Wiley & Sons, Inc.; 2010.
[42] Aasberg-Petersen K, Dybkjaer I, Ovesen CV, Schjodt NC, Sehested J, Thomsen SG. Natural gas to synthesis gas – catalysts and catalytic processes. J Nat Gas Sci Eng 2011;3(2):423–59.
[43] Liu Ming, van der Kleij A, Verkooijen AHM, Aravind PV. An experimental study of the interaction between tar and SOFCs with Ni/GDC anodes. Appl Energy 2013;108(0):149–57.
[44] Qu Zuopeng, Aravind PV, Boksteen SZ, Dekker NJJ, Janssen AHH, Woudstra N, et al. Three-dimensional computational fluid dynamics modeling of anode-supported planar SOFC. Int J Hydrogen Energy 2011;36(16):10209–20 [European fuel cell 2009].
[45] Fan L, van Biert L, Thallam Thattai A, Verkooijen AHM, Aravind PV. Study of methane steam reforming kinetics in operating solid oxide fuel cells: influence of current density. Int J Hydrogen Energy 2015;40(15):5150–9.
[46] Woolcock Patrick J, Brown Robert C. A review of cleaning technologies for biomass-derived syngas. Biomass Bioenergy 2013;52(0):54–84.
[47] LeValley Trevor L, Richard Anthony R, Fan Maohong. The progress in water gas shift and steam reforming hydrogen production technologies – a review. Int J Hydrogen Energy 2014;39(30):16983–7000.
[48] Mendes D, Mendes A, Madeira LM, Iulianelli A, Sousa JM, Basile A. The water-gas shift reaction: from conventional catalytic systems to Pd-based membrane reactors – a review. Asia-Pacific J Chem Eng 2010;5:111–37.
[49] Toonssen Richard. Sustainable power from biomass. Comparison of technologies for centralized or decentralized fuel cell systems. Technische Universiteit Delft; 2010.
[50] Sircar S, Golden TC. Purification of hydrogen by pressure swing adsorption. Sep Sci Technol 2000;35(5):667–87.
[51] Mori D, Hirose K. Recent challenges of hydrogen storage technologies for fuel cell vehicles. Int J Hydrogen Energy 2009;34(10):4569–74 [2nd World hydrogen technologies convention].
[52] Hyundai. We've reimagined the idea of an electric vehicle. Introducing the 2015. TUCSON FUEL CELL; March 2015.
[53] Toyota. Powering the future. Hydrogen fuel cell vehicles could change mobility forever; March 2015.
[54] Geersen Theo M. Physical properties of natural gas. Groningen: N.V. Netherlandse Gasunie; 1988.
[55] Geurds MJT, Huijzer EL, Hardi EE. Alternative biomathane analysis. In: International gas research conference, Seoul; 2011.
[56] Deloitte. European energy market reform. Country profile. Netherlands; 2013.
[57] The Netherlands. Energy efficiency report. The ABB Group; January 2011.
[58] The Netherlands. Energy efficiency report. ABB Group; March 2013.
[59] TU Delft. Cycle-Tempo 5.0; 2015.
[60] TU Delft. Cycle-Tempo manual. Reference guide; 2015.
[61] De Groot A. Advanced energy analysis of high temperature fuel cell systems [Ph.D. thesis]. Applied Sciences, TU Delft; 2004.
[62] Aravind PV, Woudstra T, Woudstra N, Spliethoff H. Thermodynamic evaluation of small-scale systems with biomass gasifiers, solid oxide fuel cells with Ni/GDC anodes and gas turbines. J Power Sources 2009;190(2):461–75.
[63] Liu Ming, Aravind PV, Woudstra T, Cobas VRM, Verkooijen AHM. Development of an integrated gasifier – solid oxide fuel cell test system: a detailed system study. J Power Sources 2011;196(17):7277–89 [Proceedings of 2010 European solid oxide fuel cell forum].
[64] Tsatsaronis George. Definitions and nomenclature in exergy analysis and exergoeconomics. Energy 2007;32(4):249–53 [ECOS 05. 18th international conference on efficiency, cost, optimization, simulation, and environmental impact of energy systems ECOS 05].
[65] Baehr Hans Dieter, Kabelac Stephan. Thermodynamik – Grundlagen Und Technische Anwendungen, vol. 15. Springer-Lehrbuch; 2012 [Auflage].
[66] Hall Stephen. Fans, blowers, and compressors. In: Hall Stephen, editor. Branan's rules of thumb for chemical engineers. Oxford: Butterworth-Heinemann; 2012. p. 118–33 [chapter 6].
[67] Low voltage industrial performance motors. ABB Energy; April 2014.
[68] Rostrup-Nielsen JR, Bøgild Hansen J. Steam reforming for fuel cells. In: Shekhawat Dushyant, Spivey James J, Berry David A, editors. Fuel cells. Amsterdam: Elsevier; 2011. p. 49–71 [chapter 4].
[69] Fuel Cell Technical Team. Fuel Cell Technical Team Roadmap; June 2013. <http://energy.gov/>.
[70] Eberle Ulrich, Muller Bernd, Helmolt Rittmar von. Fuel cell electric vehicles and hydrogen infrastructure: status 2012. Energy Environ Sci 2012;5:8780–98.
[71] Knoope MMJ, Guijt W, Ramirez A, Faaij APC. Improved cost models for optimizing {CO2} pipeline configuration for point-to-point pipelines and simple networks. Int J Greenhouse Gas Control 2014;22:25–46.
[72] de Bruijn FA, Dam VAT, Janssen GJM. Review: durability and degradation issues of PEM fuel cell components. Fuel Cells 2008;8(1):3–22.
[73] Stanislowski M, Froitzheim J, Niewolak L, Quadakkers WJ, Hilpert K, Markus T, et al. Reduction of chromium vaporization from SOFC interconnectors by highly effective coatings. J Power Sources 2007;164(2):578–89.
[74] Jiang San Ping, Chen Xinbing. Chromium deposition and poisoning of cathodes of solid oxide fuel cells – a review. Int J Hydrogen Energy 2014;39(1):505–31.
[75] Chatterjee Dilip, Biswas Samir. Development of chromium barrier coatings for solid oxide fuel cells. Int J Hydrogen Energy 2011;36(7):4530–9 [Emerging materials technology: materials in clean power system].
[76] Wijk Ad Van. Welcome to the green village. IOS Press BV; 2013. ISBN 978-1-61499-284-4.
[77] Accenda BV; 2016. <http://www.accenda.nl/>.
[78] Pret-a-Loger – TU Delft – Solar Decathlon house. Pre-a-Loger; 2016. <http://www.pretaloger.nl/project/>.